Neurofibromin regulates corticostriatal inhibitory networks during working memory performance

Carrie Shilyansky[a], Katherine H. Karlsgodt[b], Damian M. Cummings[c], Kyriaki Sidiropoulou[d], Molly Hardt[b], Alex S. James[b], Dan Ehninger[a], Carrie E. Bearden[b,e,f], Panayiota Poirazi[d], J. David Jentsch[b,e,f], Tyrone D. Cannon[b,e,f], Michael S. Levine[c,e,f], and Alcino J. Silva[a,b,c,e,f,1]

[a]Department of Neurobiology, University of California, Los Angeles, CA 90095; [b]Department of Psychology, University of California, Los Angeles, CA 90095; [c]Mental Retardation Research Center, The David Geffen School of Medicine, University of California, Los Angeles, CA 90095; [d]Institute of Molecular Biology and Biotechnology-Foundation for Research and Technology-Hellas (FORTH), Heraklion, 711 10 Crete, Greece; [e]Department of Psychiatry and Biobehavioral Sciences, The David Geffen School of Medicine, University of California, Los Angeles, CA 90095; and [f]Brain Research Institute, University of California, Los Angeles, CA 90095

Edited* by Richard F. Thompson, University of Southern California, Los Angeles, CA, and approved June 1, 2010 (received for review April 14, 2010)

Neurofibromatosis type I (NF1) is one of the most common single-gene causes of learning disabilities. Here, we use behavioral working memory probes and electrophysiological studies in a mouse model of NF1 (*Nf1* heterozygous null mutants; *Nf1*$^{+/-}$) to demonstrate that (*i*) Neurofibromin regulates prefrontal and striatal inhibitory networks, specifically activity-dependent GABA release and (*ii*) is required for working memory performance, with inhibition-dependent working memory deficits seen in *Nf1*$^{+/-}$ mice. We find that increased inhibition in medial prefrontal cortex (mPFC) is sufficient to alter persistent activity in a biophysical model of an mPFC microcircuit, suggesting a possible mechanism for *Nf1*$^{+/-}$ working memory deficits. Accordingly, working memory assays applied during functional MRI (fMRI) studies in human subjects with NF1 reveal hypoactivation of corticostriatal networks, which is associated with impaired working memory performance. Collectively, these integrative mouse and human studies reveal molecular and cellular mechanisms contributing to working memory deficits in NF1.

GABA | Ras | prefrontal cortex | learning disability | neurofibromatosis type I

Neurofibromatosis type 1 (NF1) is a valuable model for understanding mechanisms of learning disabilities (1). NF1 is a common genetic disorder (incidence 1:3,000) that results from mutations in a single gene (*Nf1*) that encodes the neurofibromin protein (2, 3). Specific deficits in the domains of visuospatial and executive functions are among the most common cognitive deficits associated with this syndrome (1, 4, 5). Previous mechanistic studies in a mouse model of NF1 (*Nf1* heterozygous null mutants or *Nf1*$^{+/-}$) demonstrated that neurofibromin modulates Ras-dependent GABA release in the hippocampus, which in turn modulates long-term potentiation (LTP) and hippocampal-dependent learning (6, 7). However, the mechanisms underlying frontal executive dysfunction in NF1, including prominent working memory deficits (5), are unknown. Therefore, to investigate mechanisms underlying working memory deficits associated with the NF1 mutation we carried out parallel experiments in mice and humans.

Working memory is a cognitive construct involving the ability to hold and update information transiently in mind in the service of higher-order cognitive activities. Executive functions, including working memory, are thought to depend on common corticostriatal networks (8–11). Therefore, our experiments focused on frontal corticostriatal circuitry, with an emphasis on the dorsolateral prefrontal cortex (DLPFC) in humans, thought to be critical for working memory (12), and its functionally analogous structure in rodents, the medial prefrontal cortex (mPFC) (13, 14).

Here, we report Ras-dependent increases in GABA release in the mPFC and striatum of the *Nf1*$^{+/-}$ mouse model. Increased GABAergic inhibition is likely to be responsible for the working memory deficits that we found in the *Nf1*$^{+/-}$ mice because these deficits could be reversed with a drug that decreased inhibition. Further, functional MRI (fMRI) studies in human subjects with NF1 revealed decreased neural activity in frontal corticostriatal networks in NF1 patients that correlated with their degree of working memory impairment. These convergent cross-species findings support the hypothesis that working memory deficits associated with the NF1 mutation in both mice and humans are caused by loss of neurofibromin regulation of frontal corticostriatal inhibition.

Results

***Nf1* Regulates Activity-Dependent GABA Release in Prefrontal Cortex.** The *Nf1*$^{+/-}$ mutation was previously shown to alter GABAergic inhibition in the hippocampus in mice (6, 7). Because prefrontal dysfunction could account for the prominent executive function deficits associated with NF1, we studied inhibition in mPFC of *Nf1*$^{+/-}$ mice. We focused on this area because of its homology to human DLPFC and its key role in rodent working memory tasks (14, 15). We used whole-cell patch clamp to record spontaneous synaptic activity induced by local inhibitory and excitatory networks in single neurons within layer II/III in acute slices from adult mice. Our results show that in the mPFC of *Nf1*$^{+/-}$ mice, the frequency of spontaneous inhibitory postsynaptic currents (sIPSCs) is significantly higher ($P = 0.02$) than in WT littermate controls; this increase in frequency was observed across all sIPSC amplitudes ($P < 0.001$; Fig. 1*A*). Also, analysis of the cumulative distribution of the intervals between sIPSCs confirmed an increased frequency in *Nf1*$^{+/-}$ mice ($P < 0.001$; Fig. S1*A*). In contrast, the frequency of spontaneous excitatory postsynaptic currents (sEPSCs) recorded in the same neurons is not altered in *Nf1*$^{+/-}$ mice ($P = 0.69$; Fig. 1*B*). Importantly, the *Nf1*$^{+/-}$ mutation did not affect the kinetics of either sIPSCs or sEPSCs (Fig. S1*B*) in the mPFC. Because both sIPSCs and sEPSCs were recorded in the same neurons, these data also demonstrate that the ratio of excitatory to inhibitory drive onto those neurons is abnormally low in the *Nf1*$^{+/-}$ mice.

We next examined causes of increased inhibition in the *Nf1*$^{+/-}$ mice. Specifically, we asked whether the increased inhibition in the *Nf1*$^{+/-}$ mice is caused by a cell autonomous effect of *Nf1* deletion in interneurons. To assess this directly, we used the Cre/loxP system to create *Dlx-Cre*$^{+}$;*Nf1*$^{flox/+}$ mice with a heterozygous deletion of *Nf1* restricted to inhibitory interneurons in the prefrontal cortex (7, 16). *Dlx-Cre*$^{+}$;*Nf1*$^{flox/+}$ mice show an increased frequency of sIPSCs ($P = 0.006$; Fig. 1*C*) compared with control

Author contributions: C.S., K.H.K., D.M.C., A.S.J., D.E., P.P., J.D.J., T.D.C., M.S.L., and A.J.S. designed research; C.S., K.H.K., D.M.C., K.S., and M.H. performed research; C.S., K.H.K., D.M.C., K.S., A.S.J., C.E.B., P.P., J.D.J., M.S.L., and A.J.S. analyzed data; and C.S., K.H.K., C.E.B., J.D.J., M.S.L., and A.J.S. wrote the paper.

The authors declare no conflict of interest.

*This Direct Submission article had a prearranged editor.

[1]To whom correspondence should be addressed. E-mail: silvaa@mednet.ucla.edu.

This article contains supporting information online at www.pnas.org/lookup/suppl/doi:10.1073/pnas.1004829107/-/DCSupplemental.

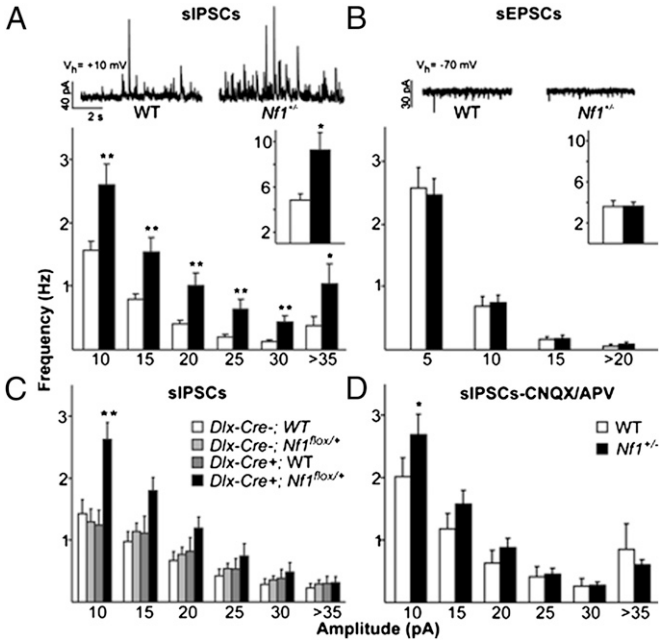

Fig. 1. Whole-cell recordings in mPFC of $Nf1^{+/-}$ mice demonstrate specific increases in inhibition. (*A*) $Nf1^{+/-}$ cells (n = 13) show increased frequency of sIPSCs compared with WT (n = 16) across all amplitude bins (RM ANOVA $P <$ 0.001; $^*P < 0.05$; $^{**}P < 0.01$, Tukey's post hoc) and in overall sIPSC frequency (*Inset* $^*P < 0.05$, t test). Representative traces of sIPSC recordings shown above. (*B*) No difference in frequency of sEPSCs is seen between $Nf1^{+/-}$ cells (n = 12) and WT (n = 13) across amplitude bins or overall (*Inset*). Representative traces of sEPSC recordings shown above. (*C*) Interneuronal *Nf1* deletion in *Dlx-Cre+*; $Nf1^{flox/+}$ cells (n = 8) leads to increased frequency of sIPSCs compared with control groups: *Dlx-Cre+*;WT (n = 9), *Dlx-Cre-*;$Nf1^{flox/+}$ (n = 14), or *Dlx-Cre-*;WT (n = 11) (P = 0.006, RM ANOVA; $^{**}P < 0.01$, Tukey's post hoc). (*D*) In the presence of glutamate receptor antagonists CNQX/APV, $Nf1^{+/-}$ cells (n = 10) show increased frequency of sIPSCs compared with WT (n = 8) across all amplitude bins (RM ANOVA P = 0.009; $^*P < 0.05$, Tukey's post hoc). Error bars represent SEM.

groups, demonstrating that *Nf1* regulates inhibitory release from mPFC interneurons. This action of *Nf1* within interneurons is confirmed pharmacologically: in the presence of CNQX(10 μM) and APV (50 μM), which blocks excitatory drive, $Nf1^{+/-}$ mice still showed a higher frequency of sIPSCs (P = 0.009; Fig. 1*D*) in mPFC. It is important to note that this difference is driven by the more frequent small amplitude sIPSCs (Fig. 1 *C* and *D*); large amplitude sIPSCs are comparatively rare, and therefore we could not determine whether their frequency is also different between mutants and controls.

We next examined how the $Nf1^{+/-}$ mutation affected interneuron function. It is possible that the increase in sIPSCs frequency is caused by activity-dependent changes, such as excitability. To address this possibility, we blocked action potentials in the slice with TTX (1 μM), and recorded miniature IPSCs (mIPSCs) in layer II/III pyramidal neurons. An analysis of the cumulative distribution of the intervals between mIPSCs revealed no differences between $Nf1^{+/-}$ mice and WT controls (P = 1; Fig. S1*C*). These data demonstrate that the increased frequency of inhibitory currents observed in $Nf1^{+/-}$ mice is activity-dependent. Cumulative amplitude distributions of mIPSCs in mPFC were also examined in TTX, and no differences between $Nf1^{+/-}$ mice and WT were found (P = 0.585; Fig. S1*C*). In combination, these experiments demonstrate that *Nf1* affects the inhibitory system most prominently by regulating activity-dependent GABAergic release in mPFC.

We next investigated molecular mechanisms by which the *Nf1* mutation leads to increased activity-dependent inhibition. Specifically, we focused on the Ras signaling pathway, as *Nf1* encodes a negative regulator of Ras signaling (neurofibromin) (17, 18), and increased Ras activity has been previously reported in prefrontal cortex of $Nf1^{+/-}$ mice (19). To study whether increased inhibition in $Nf1^{+/-}$ mice is Ras dependent, we decreased Ras signaling in mPFC slices from $Nf1^{+/-}$ mice using bath application of U0126 (10 μM). U0126 functions as a noncompetitive inhibitor of MEK, a downstream effector of Ras. A significant effect of U0126 application on sIPSC frequency (P = 0.003; Fig. 2*A*) was seen. Importantly, U0126 eliminated the difference in sIPSC frequency between genotypes (P = 0.553) that was observed before U0126 application (P = 0.028). U0126 also decreased sEPSC frequency (P = 0.012; Fig. 2*B*, *Right*), but to the same degree across genotypes (P = 0.357; Fig. 2*B*, *Left*). These data suggest that increased GABA release from inhibitory networks in $Nf1^{+/-}$ mice is Ras/MEK dependent and that neurofibromin plays an important role in inhibitory, but not excitatory neurons, to modulate Ras-dependent neurotransmitter release.

Levels of Inhibition Seen in $Nf1^{+/-}$ Mice Alter Persistent Activity in a Computational Model. As other mechanisms may be altered in $Nf1^{+/-}$ mice, we wished to further explore the significance of neurofibromin modulation of mPFC inhibitory networks. A computational approach allowed us to manipulate inhibition in isolation within a model prefrontal microcircuit in which we incorporated the background levels of sIPSCs and sEPSCs measured in $Nf1^{+/-}$ and WT mice. This allowed us to ask whether inhibitory changes seen in $Nf1^{+/-}$ mice could on their own be sufficient to significantly affect complex network properties thought to be important for working memory. We focused on the ability of prefrontal networks to sustain persistent activity following a transient stimulus, as this property is thought to be modulated by GABA-dependent inhibition (20–22), and is critical for working memory (23, 24). When using WT values for sIPSC and sEPSC frequency, persistent activity lasting more than 3 s was induced using synchronous, single pulse stimulation with a probability of 0.84 in our model microcircuit. When the frequency of background inhibitory activity was increased to levels seen in the $Nf1^{+/-}$ mPFC, the probability for induction of persistent activity was decreased by 35% (Fig. S2*A*). These results suggest that the increased inhibition seen in $Nf1^{+/-}$ prefrontal networks is sufficient to significantly alter the likelihood of ini-

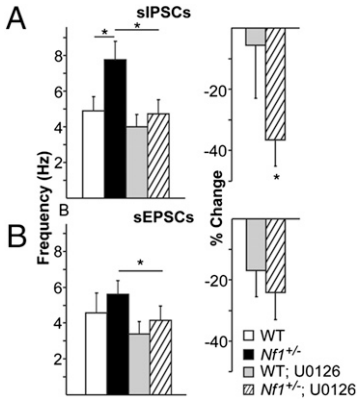

Fig. 2. Neurofibromin modulation of the Ras signaling pathway selectively regulates sIPSC frequency in mPFC. (*A Left*) U0126, an inhibitor of Ras signaling, decreases overall sIPSC frequency in both $Nf1^{+/-}$ (n = 18) and WT (n = 13) cells (RM ANOVA drug × sIPSC frequency interaction P = 0.003; $^*P < 0.05$, Tukey's post hoc). (*Right*) U0126 causes a larger within-cell decrease in sIPSC frequency in $Nf1^{+/-}$ compared with WT cells (P = 0.045, one-tailed t test) (*B Left*) U0126 decreases overall sEPSC frequency across $Nf1^{+/-}$ (n = 13) and WT (n = 8) cells (RM ANOVA drug × sEPSC frequency interaction P = 0.012; $^*P < 0.05$, Tukey's post hoc). (*Right*) Within-cell decrease in sEPSC frequency is not different between genotypes (P = 0.357, one-tailed t test). Error bars represent SEM.

tiation of persistent activity, a network property required for working memory in nonprimate and primate studies.

Increased Inhibitory Tone in Striatum of *Nf1*$^{+/-}$ Mice. In addition to prefrontal contributions to working memory, a distributed network of cortical and subcortical brain structures subserves the execution of behaviors involving working memory in nonprimate and primate studies. In particular, the striatum interacts closely with the prefrontal cortex in a circuit thought to be important for working memory (25). We therefore examined whether the *Nf1*$^{+/-}$ mice show increased inhibition in the striatum, similar to that seen in the mPFC. Whole cell recordings from medium-sized spiny neurons (MSNs) in the striatum were carried out and we analyzed frequency of sIPSCs, sEPSCs, and mIPSCs (Fig. 3 and Fig. S3). As in mPFC, frequency of sIPSCs onto MSNs is significantly higher than that seen in WT ($P < 0.001$; Fig. 3*A*), although frequency of mIPSCs is unchanged (Fig. S3*A*). In contrast, the frequency of sEPSCs recorded in the same neurons, is not different between WT and *Nf1*$^{+/-}$ mice ($P = 0.56$; Fig. 3*B*). These data indicate that the striatum of *Nf1*$^{+/-}$ mice shows an activity-dependent increase in frequency of inhibitory but not excitatory events.

Behavioral Working Memory Deficits in *Nf1*$^{+/-}$ Mice. Next, we examined the behavioral impact of increased inhibition in prefrontal cortex and striatum in *Nf1*$^{+/-}$ mice. We started by testing the mice in a behavioral task known to depend on the corticostriatal network, the delayed win-shift radial arm maze (15, 26, 27). This task is carried out in two phases such that the location of arms entered in a training phase must be maintained over a delay period and used to guide entries into unvisited arms during a testing phase. Within-phase errors during the task reflect re-entries into an arm already visited during the same phase. Prefrontal and striatal (15, 28), but not hippocampal, lesions increase these errors in the testing phase. Across-phase errors reflect entries of arms in the testing phase that were previously visited during the training phase. Throughout 10 d of delayed win-shift radial arm maze, the *Nf1*$^{+/-}$ mice showed normal training phase performance compared with WT ($P = 0.883$; Fig. 4*A*). However, in the testing phase, *Nf1*$^{+/-}$ mice showed increased total within-phase errors ($P = 0.047$; Fig. 4*B*). The increase in within-phase errors is most evident in days 1–6 of the task ($P = 0.024$; Fig. 4*D*). With three additional days of training (days 7–9), within-phase errors in the *Nf1*$^{+/-}$ mutants decreased to WT levels ($P = 0.74$). In contrast to within-phase errors, the total number of across-phase errors in the *Nf1*$^{+/-}$ group was not different from WT ($P = 0.403$; Fig. 4*C*). These data demonstrate that the *Nf1*$^{+/-}$ mice show a specific increase in within-phase errors in the testing phase of the delayed win-shift radial arm maze.

Further, this deficit is sensitive to a low dose of picrotoxin (0.025 mg/kg; i.p.), a GABA(A) receptor antagonist. Analysis of within-phase errors on the testing phase identified a differential effect of picrotoxin on *Nf1*$^{+/-}$ and WT mice across days 1–6 ($P = 0.009$; Fig. 4*E*). Importantly, the dose of picrotoxin that improved the performance of *Nf1*$^{+/-}$ mice (within-phase errors on the testing phase; $P = 0.047$) did not affect WT ($P = 0.77$). Furthermore, picrotoxin did not affect across phase errors in either genotype ($P = 0.184$; Fig. S4). This result demonstrates the behavioral specificity of the picrotoxin manipulation and provides evidence that the increased inhibition in *Nf1*$^{+/-}$ mice disrupts behavior.

Increased within-phase errors in the delayed win-shift radial arm maze could potentially reflect failures of working memory, although failure of other higher level executive functions could also contribute. To specifically address working memory function in *Nf1*$^{+/-}$ mice, we tested performance on an operant spatial delayed nonmatch to sample task (29–31). In this task, mice are given serial

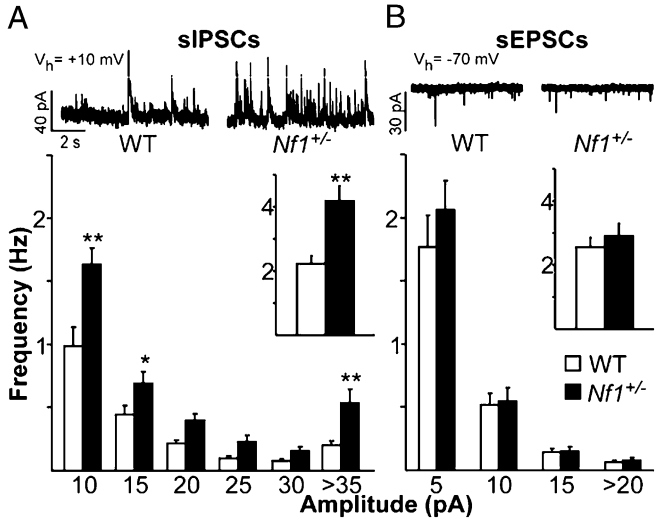

Fig. 3. Whole cell recordings of sIPSCs and sEPSCs onto cells in the striatum of *Nf1*$^{+/-}$ mice demonstrate specific increases in inhibition. (*A*) *Nf1*$^{+/-}$ MSNs ($n = 11$) show increased frequency of sIPSCs compared with WT ($n = 10$) across all amplitude bins (RM ANOVA $P < 0.001$; $^*P < 0.05$; $^{**}P < 0.01$, Tukey's post hoc) and in overall sIPSC frequency (*Inset* $^*P < 0.05$, *t* test). Representative traces of sIPSC recordings shown above. (*B*) No difference in frequency of sEPSCs is seen between *Nf1*$^{+/-}$ MSNs ($n = 10$) and WT ($n = 9$) across amplitude bins or overall (*Inset*). Representative traces of sEPSC recordings shown above. Error bars represent SEM.

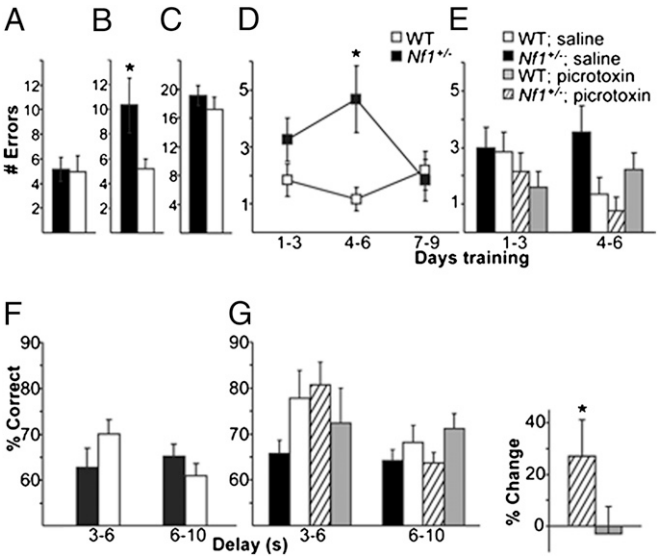

Fig. 4. Working memory impairments caused by increased inhibition in the *Nf1*$^{+/-}$ mice. (*A–C*) Delayed win-shift radial arm maze errors, summed across 10 d of task performance, are compared between *Nf1*$^{+/-}$ ($n = 12$) and WT ($n = 12$) mice for training phase errors ($P = 0.883$, *t* test), testing phase within-phase errors ($P = 0.047$, *t* test), and testing phase across-phase errors ($P = 0.403$, *t* test). (*D*) *Nf1*$^{+/-}$ mice make more testing phase within-phase errors during the first 6 d of the task (RM ANOVA genotype × day × error; $P = 0.024$, $^*P < 0.05$, Tukey's post hoc). (*E*) Picrotoxin improves within-phase errors ($P = 0.009$) in *Nf1*$^{+/-}$ mice (RM ANOVA drug × genotype × day × error). Comparisons made across four groups: saline ($n = 20$) and picrotoxin ($n = 18$) treated *Nf1*$^{+/-}$ mice and saline ($n = 20$) and picrotoxin treated WT mice ($n = 19$). (*F*) In the operant delayed nonmatch to sample task, *Nf1*$^{+/-}$ mice ($n = 12$) show impaired accuracy (RM ANOVA genotype × delay × %correct $P = 0.043$) compared with WT ($n = 10$). (*G*) Picrotoxin improves accuracy in *Nf1*$^{+/-}$ mice ($n = 11$, RM ANOVA drug × genotype × delay × %correct $P = 0.037$) compared to WT ($n = 9$). (*Left*) Accuracy of *Nf1*$^{+/-}$ and WT mice administered saline or picrotoxin (0.025 mg/kg) in a counterbalanced within-subject design. (*Right*) Within-subject percent change in accuracy at the 3–6 s delay ($^*P < 0.05$; one-tailed *t* test). Error bars represent SEM.

NEUROSCIENCE

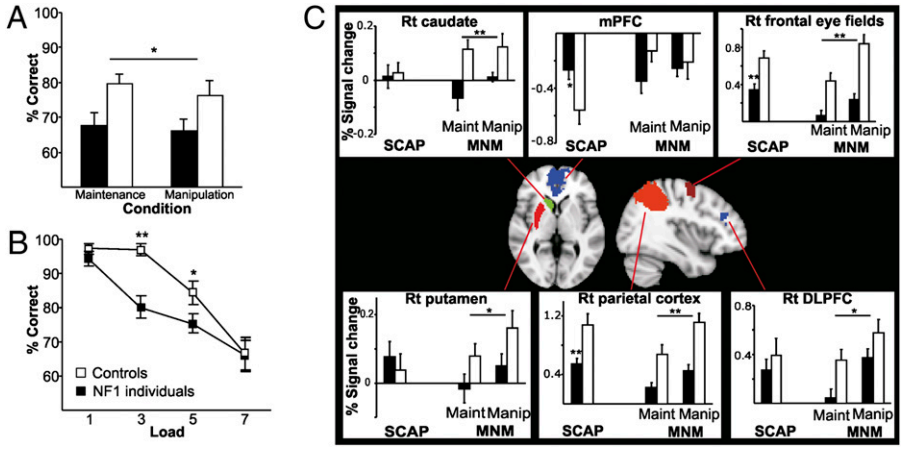

Fig. 5. Hypoactivation of corticostriatal structures and working memory deficits in NF1 individuals. (*A*) Individuals with NF1 (n = 14) show decreased testing phase accuracy in both working memory maintenance and manipulation conditions compared with age matched controls (n = 12; RM ANOVA group × % correct P = 0.019). (*B*) Individuals with NF1 show decreased testing phase accuracy in the spatial capacity task across loads (RM ANOVA group × %correct P = 0.03; *P < 0.05; **P < 0.01, Tukey's post hoc). (*C*) Center: Regions of interest in which activation was measured during performance of both the SCAP and StMNM. Individual graphs: BOLD signal changes during each task (*P < 0.05; **P < 0.01, RM ANOVA group × region). Error bars represent SEM.

trials, each consisting of two phases (sample presentation and choice) separated by a variable delay of 3–10 s. Both $Nf1^{+/-}$ and WT mice showed comparable ability to accurately respond to the cue presented in the sample phase, indicating that sensorimotor function, motivation, and response selection were normal in $Nf1^{+/-}$ mice. However, in the choice phase of delayed testing, the $Nf1^{+/-}$ mice showed an impairment (P = 0.043; Fig. 4*F*): they showed poor accuracy across all delays tested, although WT mice showed higher performance at 3–6 s delays, but significantly decreased accuracy (P = 0.02) as delays increased up to 10 s. The delay dependent performance of the WT mice suggests that working memory can support performance on this task successfully across delays up to 6 s, with performance decreasing as the task becomes more challenging. However, in $Nf1^{+/-}$ mice, working memory cannot support accurate performance, even at intervals of 3–6 s.

This working memory impairment was also improved by a low dose (0.025 mg/kg) of picrotoxin (P = 0.037; Fig. 4*G*). Picrotoxin significantly improved the pattern of performance across delays in $Nf1^{+/-}$ mice (P = 0.025) but did not affect performance of WT mice (P = 0.389). In both tasks, the dose of picrotoxin used is similar to that previously seen to improve long-term memory in WT (7). Together, these studies suggest that $Nf1^{+/-}$ mice show behavioral deficits that are related to increased inhibition and specifically affect working memory.

Working Memory-Associated Corticostriatal Dysfunction in Human NF1. Using a combination of cognitive testing and fMRI, we next determined whether human patients with NF1 also demonstrate working memory deficits related to corticostriatal dysfunction. We used two visuospatial working memory tasks that parallel the operant delayed nonmatch to sample task used with $Nf1^{+/-}$ mice and are known to activate a network of cortical and striatal brain structures (32, 33). Within the prefrontal cortex, fMRI analysis focused on the DLPFC, an area in primates that is functionally homologous to mPFC in rodents (13, 14, 34). Additionally, regions of interest (ROIs) in frontal eye fields and parietal cortex were examined, as these areas are consistently recruited during working memory tasks in human and nonhuman primates (35).

The first task assesses spatial working memory maintenance and manipulation (stMNM). NF1 individuals showed significantly lower accuracy across both the spatial working memory maintenance and manipulation conditions than controls (P = 0.019; Fig. 5*A*). During fMRI task performance, NF1 individuals showed significantly reduced neural activity relative to controls in both cortical (DLPFC, P = 0.036; frontal eye fields, P < 0.001; parietal cortex, P < 0.001; Fig. 5*C*) and striatal brain regions (caudate, P = 0.006; putamen, P = 0.015; Fig. 5*C*). Right DLPFC activation significantly predicted stMNM performance in NF1 individuals ($F_{1,11}$ = 8.69, P = 0.013; r^2 = 0.3119; Fig. 6*A*) in a robust regression analysis.

Consistent findings were observed in the second task, a parametric probe of spatial working memory capacity (SCAP) (32). NF1 individuals showed significantly lower accuracy relative to controls overall (P = 0.03; Fig. 5*B*), with a steeper decline in performance accuracy as memory load increased (P = 0.016). Using a robust regression analysis, task performance was again significantly predicted by right DLPFC activation in NF1 individuals ($F_{1,11}$ = 50.86, P < 0.001; r^2 = 0.5398; Fig. 6*B*). Additionally, NF1 individuals showed reduced neural activation compared with controls in two right-lateralized cortical areas critical for maintenance of spatial information in working memory, the right frontal eye fields (P = 0.002; Fig. 5*C*) and the right parietal cortex (P = 0.003; Fig. 5*C*). In controls, task-associated deactivation was observed in the medial PFC during task performance. However, this task-associated decrease was significantly attenuated in NF1 individuals (P = 0.020; Fig. 5*C*).

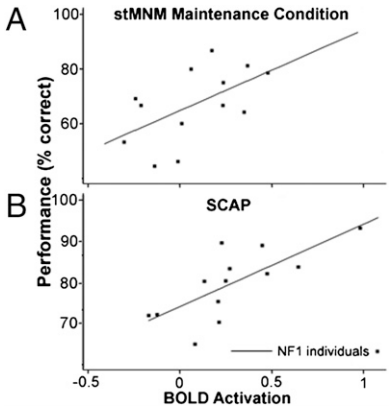

Fig. 6. Degree of DLPFC hypoactivation predicts degree of performance impairment in working memory maintenance tasks in individuals with NF1. Significant association between right DLPFC activation and task performance during (*A*) the maintenance condition of the MNM task ($F_{1,11}$ = 8.69, P = 0.013; r^2 = 0.32) and (*B*) the SCAP task ($F_{1,11}$ = 50.86, P < 0.001; r^2 = 0.54).

Overall, during SCAP performance, patients with NF1 evidenced abnormal regulation of prefrontal and related cortical structures.

As predicted by our mouse studies, our human studies indicate that blunted activation of corticostriatal networks, normally recruited during spatial working memory performance, is directly related to working memory impairments characteristic of NF1.

Discussion

Here, we report convergent evidence from parallel studies in transgenic mice and human patients regarding the mechanisms underlying working memory deficits associated with Nf1 mutations. A key finding in the $Nf1^{+/-}$ mouse experiments is that neurofibromin is an important molecular regulator of interneuronal activity in the prefrontal cortex and striatum, brain regions critical for working memory performance. The convergence between our mouse behavioral, electrophysiological, and computational modeling results indicate that the increased inhibition observed in $Nf1^{+/-}$ mice disrupts corticostriatal activity and contributes to working memory deficits, a conclusion supported by an extensive literature that connects inhibition to working memory. These data highlight the importance of neurofibromin signaling to function of corticostriatal inhibitory networks during behavior, specifically during working memory in the $Nf1^{+/-}$ mice.

Our studies in human patients reveal striking convergence with findings in $Nf1^{+/-}$ mice. With working memory tasks highly homologous to those used in mice, we find that loss of neurofibromin is associated with corticostriatal dysfunction and that this dysfunction is directly correlated with working memory deficits. Performing parallel experiments across species offers the unique opportunity to gain deeper insight into the basis of neural changes seen using in vivo neuroimaging studies in humans. In particular, our convergent cross-species findings suggest that hypoactivation of corticostriatal structures, observed with fMRI in NF1 patients, may be caused by increased GABA(A) receptor signaling. Similar effects have been noted in other fMRI studies of healthy subjects given GABA(A) agonists (36). By directly examining parallel effects of *Nf1* mutations across species in homologous neuronal circuits and behavioral tasks, we provide evidence that neurofibromin/Ras signaling in both mice and humans regulates working memory by modulating inhibition in prefrontal cortical and striatal networks.

Interestingly, altered inhibition relative to excitation has been seen in other animal models of neurodevelopmental disorders in which corticostriatal hypoactivation and working memory deficits are also found. For example, working memory deficits have been demonstrated in Down's syndrome (37, 38), Fragile X (39), and Turner syndrome (40). These deficits were associated with corticostriatal hypoactivation in fMRI studies of individuals with Fragile X (39) and Turner's syndrome (40). Animal models of these disorders have identified altered regulation of inhibition. Both Rett syndrome (*Mecp2* mutant mice) (41) and Down's syndrome (Ts65Dn mice) (42) animal models show increased inhibitory drive. The Fragile X animal model (*Fmr1* knockout mice) shows reduced excitatory drive onto cortical GABAergic interneurons (43) as well as increased GABAergic inhibition in striatum (44). Taken together, these studies of other neurodevelopmental disorders are consistent with our findings in NF1. Across these models, abnormal inhibition alters multiple synaptic properties, from cortical UP states in the Fragile X mice to hippocampal LTP in the Ts65Dn mice (42). Within each disorder, inhibition-dependent changes likely interact with other molecular mechanisms affected by the disease (for example, enhanced responses to mGluR in Fragile X) (45) to generate cognitive symptoms. Our findings indicate that working memory has conserved and homologous underpinnings in both mouse and humans that could be leveraged to further study the complex molecular and cellular mechanisms disrupted by genetic mutations associated with developmental learning disabilities.

Methods

Animal Subjects. $Nf1^{+/-}$ and WT mice, as well as *Dlx-Cre*$^{+}$;$Nf1^{flox/+}$ and their control littermates, were on a hybrid background of C57BL/6NTac and 129T2/SvEmsJ. *Dlx-Cre*$^{+}$;$Nf1^{flox/+}$ mice and controls were from a cross between a line expressing Cre under the *Dlx* promoter and a line expressing a floxed *Nf1* allele (46). All experiments used littermates as controls and were done with the experimenter blinded to genotype. Behavioral experiments were conducted with animals food-deprived to 85% of their starting weight. Behavior and electrophysiology was carried out on mice of the same age range (3–8 mo old).

Animal Studies. Whole-cell patch-clamp recordings were made in acute slices containing mPFC or striatum as previously described (47). Event detection was carried out off-line using MiniAnalysis software. Threshold for event detection was set above the root mean square noise level (usually 10 pA for sIPSCs, 5 pA for sEPSCs). Analysis was carried out blind to genotype.

Delayed win-shift radial arm maze task was carried out on an eight arm apparatus. Access to each arm from a central platform was regulated by a guillotine door. Reward pellets (14 mg grain based pellet; Bio-Serv) were placed at the end of each arm. Mice were habituated to the apparatus for 2 d. The task consisted of one training phase, followed by a 2-min delay, followed by a testing phase. The training phase required mice to make single entries into four baited arms. The testing phase required mice to make single entries into new arms that were not visited during the training phase. This series was run once per mouse per day for 10 d. The delayed nonmatch to sample task was adapted from procedures previously described in mice (31). During training on the nonmatch to sample rule, two WT mice failed to meet the criterion level of 70% correct responding and were subsequently dropped from further testing. Picrotoxin and saline injections were carried out in the home cage 20 min before start of the training phase.

Biophysical Model. The compartmental model of a layer II/III PFC pyramidal neuron was implemented in the NEURON simulation environment (48) and consisted of five compartments. The model was validated against experimental data recorded in this study (Fig. S2 *C–E*). Four pyramidal model neurons were connected in a recurrent circuit that also included one interneuron. Background inhibition and excitation in the model is based on experimental data described within this paper. Persistent activity was induced by providing a synchronous, single pulse stimulation of 40 synapses on the proximal dendrite of each model pyramidal neuron. The arrangement of these synapses varied randomly during 100 repetition trials.

Human Subjects. Fourteen individuals with NF1 and 12 controls with comparable demographics (Table S1) were recruited. A standard neuropsychological battery was performed (Table S2). NF1 and control individuals were recruited via advertisement and provided written consent for participation, as approved by the institutional review board of the University of California, Los Angeles, CA. NF1 individuals had been previously diagnosed by a physician with NF1; diagnoses were confirmed by clinical interview. Controls did not have Axis-I psychiatric or neurological disorders as assessed by the Structured Clinical Interview for DSM-IV. Exclusion criteria were significant and habitual substance use in the last 6 mo, history of head injury, mental retardation (IQ less than 70), and insufficient fluency in the English language.

Human Behavioral Task Paradigms. Study participants performed two spatial delayed response tasks, one contrasting maintenance and manipulation of spatial memoranda consisting of arrays of three dots [stMNM (32, 33)] and the other assessing parametrically increasing memory loads [SCAP (33)] consisting of arrays of increasing numbers of dots. Behavioral data were analyzed in SPSS, using repeated measures ANOVA.

fMRI Methods. All scans were acquired on a 3T Siemens Allegra scanner at University of California, Los Angeles, CA. Functional slices used an echo planar (EPI) sequence (TR/TE 3000/45 ms, 90° flip angle, 33 3-mm slices). A T2-weighted image for anatomical registration (TR/TE 5000/33 ms, 33 3-mm slices with 1-mm gap, 128 × 128 matrix, 200-mm FOV) was taken in the same AC-PC aligned plane as the functional scans. SCAP consisted of 180 scans with duration of 9 min; stMNM consisted of 256 scans with duration of 12 min, 45-s image analysis was performed in FMRIB's Software Library v 3.3 (FSL) (49). Individual subject analyses were carried out using FMRI Expert Analysis Tool (FEAT). EPI data were corrected for motion, spatially smoothed (5-mm FWHM Gaussian

kernel), high pass filtered (72 s) and then registered, first to the subject's individual T2-image, then to the MNI-152 brain (50, 51). Time-series statistical analysis was carried out using FMRIB's Improved Linear Model (FILM). Each condition was modeled for stMNM; each load was modeled separately for SCAP, with motion included as a covariate. Group analysis was carried out using FMRIB's Local Analysis of Mixed Effects (FLAME) (49, 52).

ROI Analysis. Functionally defined ROIs were created in the MNI-152 standard brain space. Using Featquery (http://www.fmrib.ox.ac.uk/fsl/feat5/featquery.html) the motion corrected, smoothed, and filtered data across each ROI was probed for percent signal change from baseline. To control for performance, the stMNM analysis contained only correct trials. The SCAP analysis used performance matched loads (80%, load 3, NF1 and 84%, load 5, control). For the SCAP, unpaired *t* tests were performed between groups. For the stMNM, repeated measures ANOVA were performed. To assess the relationship between BOLD activation and working memory performance, a robust regression was performed in Stata (v 8) for each task with functional activation in the right DLPFC predicting accuracy (percent correct). Subjects with high studentized residuals (>2) were excluded (one patient in each case).

Additional description of procedures is available in *SI Text*.

ACKNOWLEDGMENTS. We thank the individuals who participated in our behavioral and fMRI study. C.S. is supported by the Children's Tumor Foundation Young Investigators Award, Achievement Rewards for College Scientists Foundation, and National Institutes of Health Molecular and Cellular Neurobiology Training Grant 2T32MH019384-11A2. This work was supported by grants from the National Institutes of Health (2 R01 MH084315-10), Neurofibromatosis Inc., the Children's Tumor Foundation, the US Army (W81XWH-06-1-0174; to A.J.S.), and the National Institute of Mental Health (R34 MH089299-01; to C.E.B.).

1. Krab LC, et al. (2008) Impact of neurofibromatosis type 1 on school performance. *J Child Neurol* 23:1002–1010.
2. Viskochil D, et al. (1990) Deletions and a translocation interrupt a cloned gene at the neurofibromatosis type 1 locus. *Cell* 62:187–192.
3. Wallace MR, et al. (1990) Type 1 neurofibromatosis gene: Identification of a large transcript disrupted in three NF1 patients. *Science* 249:181–186.
4. Hyman SL, Shores A, North KN (2005) The nature and frequency of cognitive deficits in children with neurofibromatosis type 1. *Neurology* 65:1037–1044.
5. Rowbotham I, Pit-ten Cate IM, Sonuga-Barke EJ, Huijbregts SC (2009) Cognitive control in adolescents with neurofibromatosis type 1. *Neuropsychology* 23: 50–60.
6. Costa RM, et al. (2002) Mechanism for the learning deficits in a mouse model of neurofibromatosis type 1. *Nature* 415:526–530.
7. Cui Y, et al. (2008) Neurofibromin regulation of ERK signaling modulates GABA release and learning. *Cell* 135:549–560.
8. Bajenaru ML, et al. (2003) Optic nerve glioma in mice requires astrocyte Nf1 gene inactivation and Nf1 brain heterozygosity. *Cancer Res* 63:8573–8577.
9. Tisch S, Silberstein P, Limousin-Dowsey P, Jahanshahi M (2004) The basal ganglia: Anatomy, physiology, and pharmacology. *Psychiatr Clin North Am* 27:757–799.
10. Powell KB, Voeller KK (2004) Prefrontal executive function syndromes in children. *J Child Neurol* 19:785–797.
11. Godefroy O (2003) Frontal syndrome and disorders of executive functions. *J Neurol* 250:1–6.
12. Fuster JM, Alexander GE (1971) Neuron activity related to short-term memory. *Science* 173:652–654.
13. Brown VJ, Bowman EM (2002) Rodent models of prefrontal cortical function. *Trends Neurosci* 25:340–343.
14. Uylings HB, Groenewegen HJ, Kolb B (2003) Do rats have a prefrontal cortex? *Behav Brain Res* 146:3–17.
15. Taylor CL, Latimer MP, Winn P (2003) Impaired delayed spatial win-shift behaviour on the eight arm radial maze following excitotoxic lesions of the medial prefrontal cortex in the rat. *Behav Brain Res* 147:107–114.
16. Stühmer T, Puelles L, Ekker M, Rubenstein JL (2002) Expression from a Dlx gene enhancer marks adult mouse cortical GABAergic neurons. *Cereb Cortex* 12:75–85.
17. Ballester R, et al. (1990) The NF1 locus encodes a protein functionally related to mammalian GAP and yeast IRA proteins. *Cell* 63:851–859.
18. Xu GF, et al. (1990) The catalytic domain of the neurofibromatosis type 1 gene product stimulates ras GTPase and complements ira mutants of S. cerevisiae. *Cell* 63: 835–841.
19. Li W, et al. (2005) The HMG-CoA reductase inhibitor lovastatin reverses the learning and attention deficits in a mouse model of neurofibromatosis type 1. *Curr Biol* 15: 1961–1967.
20. Rao SG, Williams GV, Goldman-Rakic PS (2000) Destruction and creation of spatial tuning by disinhibition: GABA(A) blockade of prefrontal cortical neurons engaged by working memory. *J Neurosci* 20:485–494.
21. Constantinidis C, Williams GV, Goldman-Rakic PS (2002) A role for inhibition in shaping the temporal flow of information in prefrontal cortex. *Nat Neurosci* 5: 175–180.
22. Sawaguchi T, Matsumura M, Kubota K (1989) Delayed response deficits produced by local injection of bicuculline into the dorsolateral prefrontal cortex in Japanese macaque monkeys. *Exp Brain Res* 75:457–469.
23. Funahashi S, Bruce CJ, Goldman-Rakic PS (1993) Dorsolateral prefrontal lesions and oculomotor delayed-response performance: Evidence for mnemonic "scotomas". *J Neurosci* 13:1479–1497.
24. Funahashi S, Bruce CJ, Goldman-Rakic PS (1989) Mnemonic coding of visual space in the monkey's dorsolateral prefrontal cortex. *J Neurophysiol* 61:331–349.
25. Chudasama Y, Robbins TW (2006) Functions of frontostriatal systems in cognition: Comparative neuropsychopharmacological studies in rats, monkeys and humans. *Biol Psychol* 73:19–38.
26. Floresco SB, Braaksma DN, Phillips AG (1999) Thalamic-cortical-striatal circuitry subserves working memory during delayed responding on a radial arm maze. *J Neurosci* 19:11061–11071.
27. Floresco SB, Seamans JK, Phillips AG (1997) Selective roles for hippocampal, prefrontal cortical, and ventral striatal circuits in radial-arm maze tasks with or without a delay. *J Neurosci* 17:1880–1890.
28. Seamans JK, Floresco SB, Phillips AG (1995) Functional differences between the prelimbic and anterior cingulate regions of the rat prefrontal cortex. *Behav Neurosci* 109:1063–1073.
29. Aarde SM, Jentsch JD (2006) Haploinsufficiency of the arginine-vasopressin gene is associated with poor spatial working memory performance in rats. *Horm Behav* 49: 501–508.
30. Chudasama Y, Robbins TW (2004) Dopaminergic modulation of visual attention and working memory in the rodent prefrontal cortex. *Neuropsychopharmacology* 29: 1628–1636.
31. Jentsch JD, et al. (2009) Dysbindin modulates prefrontal cortical glutamatergic circuits and working memory function in mice. *Neuropsychopharmacology* 34:2601–2608.
32. Glahn DC, et al. (2002) Maintenance and manipulation in spatial working memory: Dissociations in the prefrontal cortex. *Neuroimage* 17:201–213.
33. Cannon TD, et al. (2005) Dorsolateral prefrontal cortex activity during maintenance and manipulation of information in working memory in patients with schizophrenia. *Arch Gen Psychiatry* 62:1071–1080.
34. Moghaddam B, Homayoun H (2008) Divergent plasticity of prefrontal cortex networks. *Neuropsychopharmacology* 33:42–55.
35. Rawley JB, Constantinidis C (2009) Neural correlates of learning and working memory in the primate posterior parietal cortex. *Neurobiol Learn Mem* 91:129–138.
36. Menzies L, et al. (2007) Effects of gamma-aminobutyric acid-modulating drugs on working memory and brain function in patients with schizophrenia. *Arch Gen Psychiatry* 64:156–167.
37. Lanfranchi S, Carretti B, Spanò G, Cornoldi C (2009) A specific deficit in visuospatial simultaneous working memory in Down syndrome. *J Intellect Disabil Res* 53:474–483.
38. Lanfranchi S, Jerman O, Vianello R (2009) Working memory and cognitive skills in individuals with down syndrome. *Child Neuropsychol* 15:397–416.
39. Kwon H, et al. (2001) Functional neuroanatomy of visuospatial working memory in fragile X syndrome: Relation to behavioral and molecular measures. *Am J Psychiatry* 158:1040–1051.
40. Haberecht MF, et al. (2001) Functional neuroanatomy of visuo-spatial working memory in Turner syndrome. *Hum Brain Mapp* 14:96–107.
41. Dani VS, et al. (2005) Reduced cortical activity due to a shift in the balance between excitation and inhibition in a mouse model of Rett syndrome. *Proc Natl Acad Sci USA* 102:12560–12565.
42. Fernandez F, et al. (2007) Pharmacotherapy for cognitive impairment in a mouse model of Down syndrome. *Nat Neurosci* 10:411–413.
43. Gibson JR, Bartley AF, Hays SA, Huber KM (2008) Imbalance of neocortical excitation and inhibition and altered UP states reflect network hyperexcitability in the mouse model of fragile X syndrome. *J Neurophysiol* 100:2615–2626.
44. Centonze D, et al. (2008) Abnormal striatal GABA transmission in the mouse model for the fragile X syndrome. *Biol Psychiatry* 63:963–973.
45. Bear MF, Dölen G, Osterweil E, Nagarajan N (2008) Fragile X: Translation in action. *Neuropsychopharmacology* 33:84–87.
46. Zhu Y, et al. (2001) Ablation of NF1 function in neurons induces abnormal development of cerebral cortex and reactive gliosis in the brain. *Genes Dev* 15:859–876.
47. Cummings DM, et al. (2009) Alterations in cortical excitation and inhibition in genetic mouse models of Huntington's disease. *J Neurosci* 29:10371–10386.
48. Hines ML, Carnevale NT (1997) The NEURON simulation environment. *Neural Comput* 9:1179–1209.
49. Smith SM, et al. (2004) Advances in functional and structural MR image analysis and implementation as FSL. *Neuroimage* 23 (Suppl 1):S208–S219.
50. Jenkinson M, Smith S (2001) A global optimisation method for robust affine registration of brain images. *Med Image Anal* 5:143–156.
51. Jenkinson M, Bannister P, Brady M, Smith S (2002) Improved optimization for the robust and accurate linear registration and motion correction of brain images. *Neuroimage* 17:825–841.
52. Behrens TE, et al. (2003) Non-invasive mapping of connections between human thalamus and cortex using diffusion imaging. *Nat Neurosci* 6:750–757.